Available online at www.sciencedirect.com

ScienceDirect

Ceramics International 42 (2016) 7571–7575

CERAMICS INTERNATIONAL

www.elsevier.com/locate/ceramint

Preparation and characterization of nanostructured titanium nitride thin films at room temperature

F. Solis-Pomar[a], O. Nápoles[b], O. Vázquez Robaina[b], C. Gutierrez-Lazos[a], A. Fundora[b], Angel Colin[a], E. Pérez-Tijerina[a], M.F. Melendrez[c,*]

[a]Facultad de Ciencias Físico-Matemáticas, Universidad Autónoma de Nuevo León, San Nicolás de los Garza, Nuevo León 66451, Mexico
[b]Instituto de Ciencias y Tecnología de Materiales (IMRE), Universidad de La Habana, San Lázaro y L, Vedado 10400, Cuba
[c]Advanced Nanocomposites Research Group (GINA), Hybrid Materials Laboratory (HML), Department of Materials Engineering (DIMAT), Faculty of Engineering, University of Concepcion, 270 Edmundo Larenas, Box 160-C, Concepcion 4070409, Chile

Received 26 November 2015; accepted 23 January 2016
Available online 29 January 2016

Abstract

Nanostructured TiN thin films were grown by reactive magnetron sputtering deposition on Si (100) substrate at room temperature. The nanostructured TiN thin films were characterized by X-ray Diffraction (XRD), X-ray Photoelectron Spectroscopy (XPS), Scanning Electron Microscopy (SEM), Scanning Tunneling Microscopy (STM), Atomic Force Microscopy (AFM), resistivity and hydrophobicity tests. The nanostructured TiN thin films had an average grain size 4.6 nm, an average roughness of 1.3 nm, a preferential orientation in the [111] direction and also they showed hydrophobicity Type I.
© 2016 Elsevier Ltd and Techna Group S.r.l. All rights reserved.

Keywords: Nanostructures; Thin films; Titanium nitride; Room temperature

1. Introduction

Within the coatings with high demand and impact on the industrial sector, are those for surface hardening of a material [1]. These have allowed conventional materials such as steel, which can be used efficiently to increase the lifetime of a part or working tool. In addition to their use in hardening of the surface of various materials, they show a high chemical stability in corrosive environments [2], high electrical conductivity values [3], high melting point [4] and infrared reflectance [5]. The first synthetic nitride hard coatings were binary titanium materials (TiN) and titanium carbide (TiC). Later developments were based on multiple coatings or multilayer where high values of hardness of the coating is obtained by varying the thickness and number of layers deposited [6], and currently are held in nanostructured coatings where the matrix of the coating consists of hard materials with nanoscale dimensions and other components such as metals and carbon are added. In terms of their hardness, these coatings are divided into two groups: hard, with hardness less than 40 GPa, and superhard, with a greater hardness than 40 GPa [7].

Among the best-known hard coating is titanium nitride. This is characterized by hardness values exceeding 24.7 GPa [4], this property is highly exploited in industry where you need coating materials or objects such as drills, bone implants, nails, blades and bearings under extreme working conditions [6,8,9]. TiN despite is being one of the first synthetic hard coatings whose mechanical properties has been widely reported in the literature for thicknesses in the order of micrometers [9], continue to be studied as shown in current research [10–12], this interest is due to the emergence of novel properties at the nanoscale that opens a range of new applications.

Recent research has revealed a dependency between the resistance of TiN_x $(0.55 < x < 1.05)$ coatings and the

*Corresponding author. Tel.: +56 41 2203187; fax: +56 41 2203391.
E-mail address: mmelendrez@udec.cl (M.F. Melendrez).

http://dx.doi.org/10.1016/j.ceramint.2016.01.164
0272-8842/© 2016 Elsevier Ltd and Techna Group S.r.l. All rights reserved.

parameters set during the manufacture as the substrate temperature, deposition time, pressure and gas flow, studying the influence parameters for glass substrates, silicon and silicon oxide [13]. Based on these results the optimum conditions for low electrical resistivity in TiN, the substrate temperature must be above 200 °C, the period of exposure of the substrate to the plasma must be 120 min or more, and the gas pressure must not exceed 4 militorr.

Given these results it appears that the grain size is not an important factor on the hardness of the material, instead the crystallographic orientation and density are determining factors [14]. These publications links the results obtained by analyzing the X-ray diffraction with the anisotropy of the material properties respect to the crystallographic directions of growth [15], from which it is concluded that the TiN_x presents greater hardness along the crystallographic direction [111] to the addresses [200] and [220], respectively.

The main goal of our work is the preparation and characterization of nanostructured thin films of titanium nitride by sputtering in substrates of Si (100) at room temperature.

2. Experimental details

The nanostructured titanium nitride (TiN) thin films were deposited on Si (100) substrates by reactive magnetron sputtering of a Ti target in an Ar/N_2 mixture at room temperature. The synthesis conditions employed for the nanostructured TiN thin films are listed in Table 1. The deposition was made using a gas mixture containing argon (Ar) and nitrogen (N_2), where Ar and N_2 were the working and reactive gases, respectively. High purity Ar (99.999%) and N_2 (99.999%) were employed for TiN depositions. The chamber was pumped down to a base pressure of 5×10^{-6} Torr before nitrogen and Ar were introduced. The flow rate of N_2 and Ar during deposition was controlled using gas flow meters. A source of DC Sputtering Ion Magnetron Materials Science Inc was used. The pre-used vacuum evaporation was performed using two pumps, mechanical JEOL 75G and RP-250 Turbo Macrotorr turbomolecular V, the gas pressure was established using a flow meter AERA FC-7800 CD.

For structural analysis of the coatings studied, the samples were analyzed through X-ray diffraction at room temperature using a PANALYTICAL EMPYREAN diffractometer with copper radiation (45 kV and 40 mA, $\lambda = 1.5406$ Å). SEM images were obtained by a microscope FEI Nova model NanoSEM 200. AFM images were obtained by a microscope Digital CP-II, STM images were obtained with a voltage of 150 mV, a current of 0.8 nA and frequencies of 3 and 5 Hz. To study the hydrophobicity, a conventional microscope was used to obtain photographs and the material was atomized with distilled water and the images were processed using Corel Draw Graphics Suite 12 to measure contact angles of droplets in the surface.

3. Results and discussion

The Fig. 1 shows the x-rays diffraction patterns of the TiN samples showing four main peaks (111), (200), (220) and (311) whit a high peak oriented in the (111) revealing the formation of a cubic face-centered structure (according to the crystallographic chart (98-008-3902). The main phase was indexed as stoichiometric TiN with space group Fm-3m. Table 2 shows the lattice parameters of the samples.

It can be seen that the growth of the nanostructured TiN thin films obtained by the technique of sputtering at room temperature, considering that the energy of particles in plasma, was sufficient to promote the formation of crystalline structures on the Si substrate (100). The results obtained are similar as those shown in the literature, where the used substrates were heated above 350 °C for the formation of the crystalline structure of the material [14,16,17]. On the other hand, Fig. 2 shows the XPS survey spectra of the TiN films exhibiting the characteristic Ti2s, Ti2p, N1s, and O1s peaks at the corresponding binding energies 563.6, 457.7, 397.0 and 531.8 eV respectively. The Ti 2p3/2 peak included two components, TiON and TiN phase. The Ti 2p1/2 458.2 eV associated with the TiO_2 phase. The spectrum of N1s peak includes two components which are

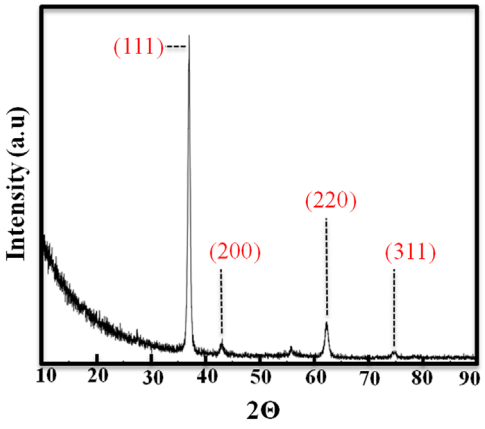

Fig. 1. XRD Diffraction patterns of nanostructured TiN samples on Si (100) by DC sputtering at room temperature.

Table 2
Lattice parameter of the samples.

Substrate	Sample	$a_{teóric}$ (Å)	a_o (Å)
Si (100)	TiN	4.27	4.22

Table 1
Synthesis conditions of nanostructure TiN thin films on Si (100) substrate by DC magnetron sputtering.

Substrate	TSub (°C)	t (min)	Ar flow (sccm)	N_2 flow (sccm)	I (mA)	V (V)	P (mT)	d_{taget} (cm)	P (W)
Si (100)	21	5	30	5	500	392	3.8	5	200

centered at 496.9 and 396 eV that can be associate these components with N–C and N–O bonding state and 398.5 (N4) eV for TiN and TiON, respectively. The O1s peak includes two components, which are centered at 529.9 and 532.2 eV that can be associate to the Ti–O bonding state and C–O, H_2O [18,19].

Fig. 3 shows the morphology of the nanostructured TiN thin films obtained by sputtering. The growth was uniform in the entire sample showing a nanostructured surface. This was corroborated by the STM tunnel effect microscopy as shown in Fig. 4. SEM micrographs taken on the surface of TiN samples on substrates of Si (100) prepared by sputtering at room temperature show a compact columnar growth as shown in Fig. 4. It was determined that by this technique the monolayers of material growth at 3.7×10^{-1} nm/s. In the SEM micrographs (Fig. 3) could be observed that the growth is shaped islands due to the adsorption energy is less than the energy required to form bonds, then the arriving atoms tend to condense to form small groups as predicted in the theoretical model of Back–Webber. This is usually the case of many metals evaporated on insulating materials. Fig. 4 shows the STM micrographs on nanostructured TiN thin films on the surface of Si (100), it confirms the column type growth for the formation of agglomerates of nanoparticles and TiN islands.

Fig. 5 shows the AFM micrographs of the nanostructured TiN thin films; they were granular with some evidence for surface roughness as shown in the Figure. The average grain

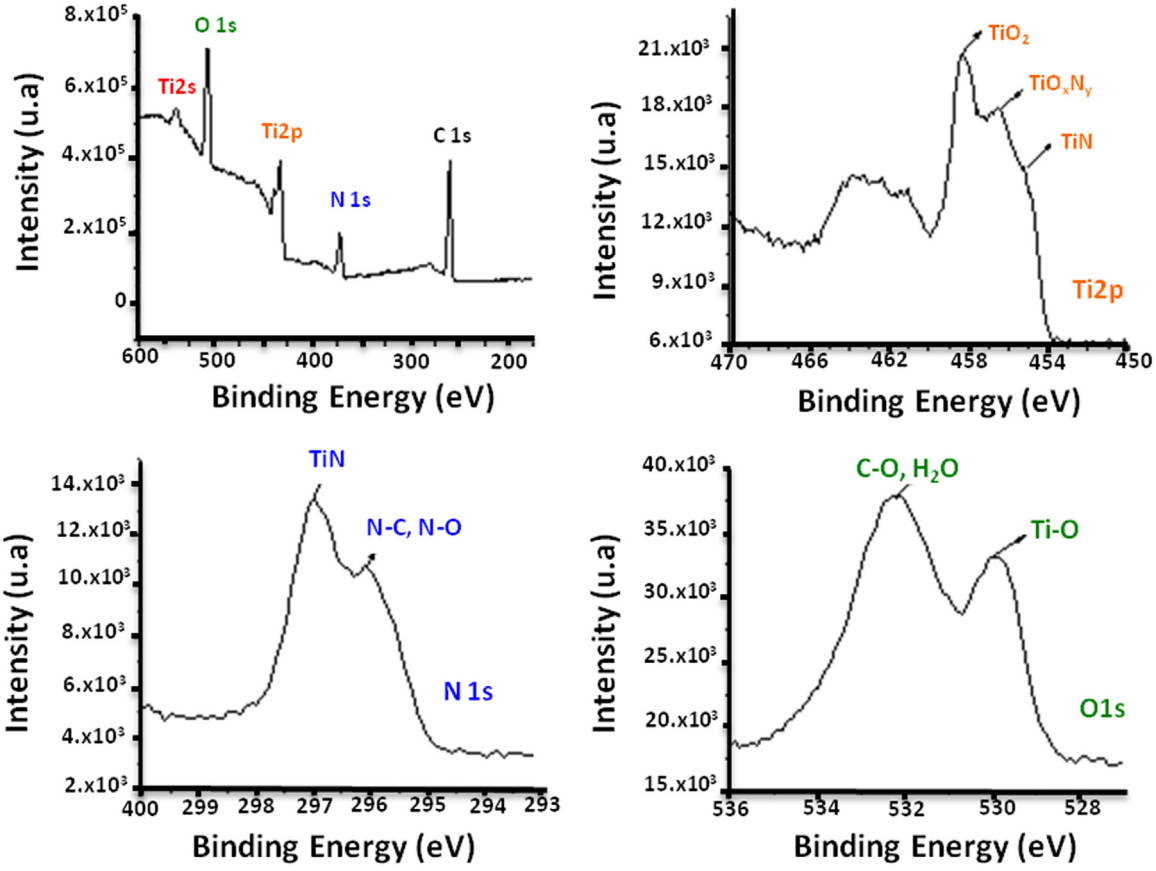

Fig. 2. High resolution XPS spectra of the TiN. (a) Survey spectra (b) Ti2p (c) N1s (d) O1s.

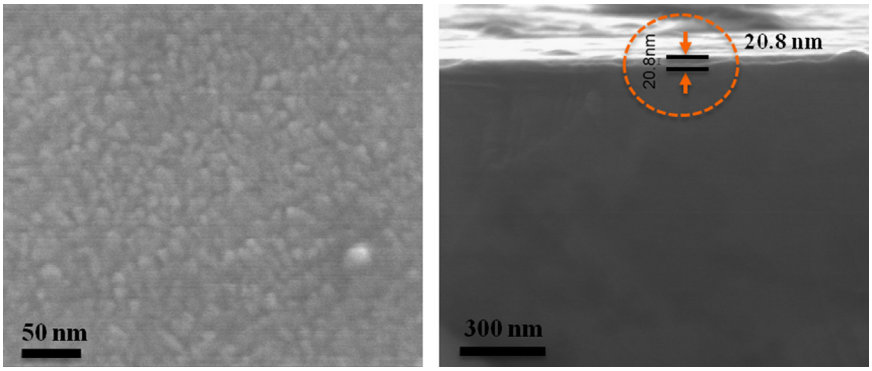

Fig. 3. SEM micrographs of the nanostructured TiN samples on Si (100) obtained by DC sputtering.

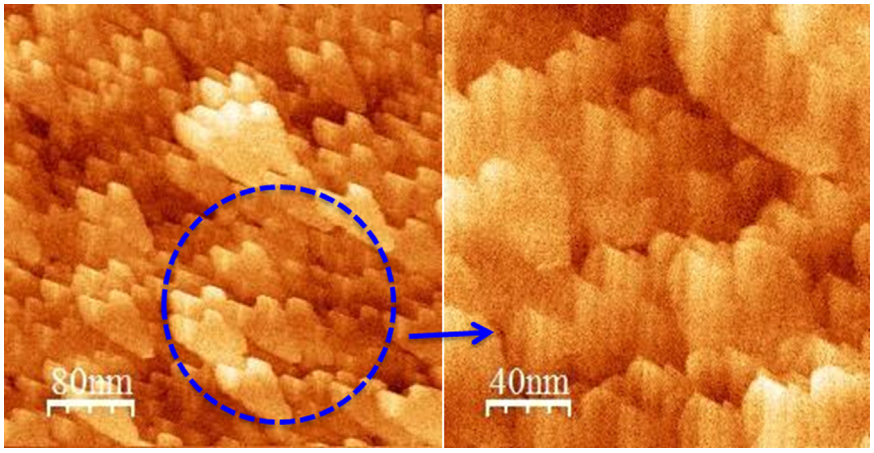

Fig. 4. STM micrographs on the surface of nanostructured TiN samples on Si (100) by DC sputtering.

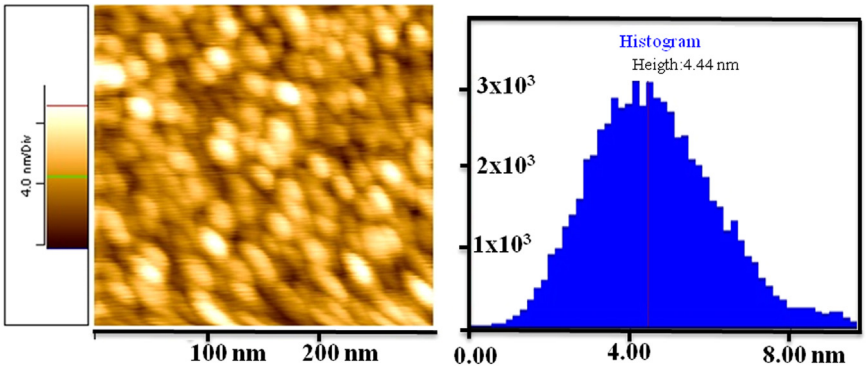

Fig. 5. AFM micrograph the surface of nanostructured TiN samples on Si (100) by DC sputtering and its distribution curve.

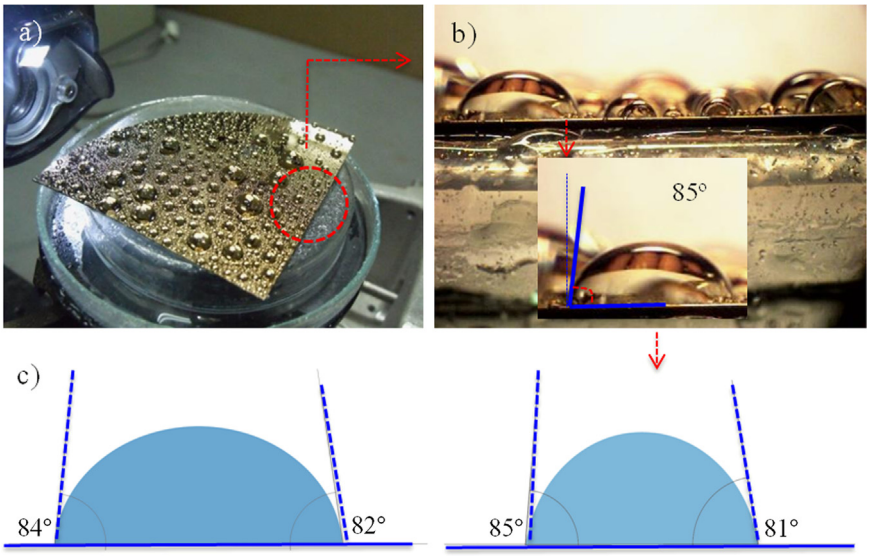

Fig. 6. Photographs of the drops formed by distilled water on the surface of nanostructured TiN/Si (100).

size was 4.60 nm with average roughness of 1.26 nm that can be due to the nanostructured crystalline growth. An experiment was made to determine the hydrophobicity of the nanostructured TiN thin films, the image of Fig. 6 shows a well-defined droplet due to the surface tension of water is higher than the interface tension of liquid–solid formed. Fig. 6b shows the distribution of droplets of different sizes and Fig. 6c shows the average contact angles of 20 drops taken randomly from two different experiments, obtaining angles above 80° for distilled water drops on the surface of TiN/Si (100). According to the standards, these TiN coatings are hydrophobic Type I [20].

The Fig. 7 shows the curve of R vs. T of the nanostructured TiN thin films. The high electrical conductivity of nanostructured TiN thin film makes them suitable for applications in the

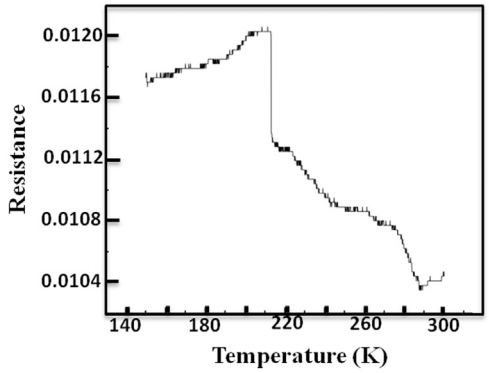

Fig. 7. *R* vs. *T* curve of TiN samples on Si (100) by DC sputtering.

semiconductor industry as diffusion barriers and interconnectors in ultra-large-scale integrated circuits and it is also suitable for thin film resistor in monolithic microwave integrated circuits [21,22]. The resistivity decreases exponentially with respect to temperature tending to have a metallic behavior. Which can be attributed to the nanostructuring of TiN films on Si (100). The temperature dependence of the conductivity of TiN films studied is exponential and exhibits a break for the films at 212 K. Elucidation of the nature of this anomaly requires additional investigations. The nature of electrical conductivity of TiN can be attributed to the intersection of the valence band of the (Ti 3d) electrons with the Fermi level. Band structure calculations show that the bonding contains a significant amount of ionic character and indicate charge transfer from the metal to the non-metal atoms upon compound formation. The charge transfer from the metal atoms is the largest at stoichiometric composition and it decreases with increasing amount of non-metal vacancies (observed in Fig. 2). Thus, the origin of the conductivity in TiN from the perspective of electronic band structure is well understood. It is clear from the results that the conductivity in nanostructured titanium nitride thin films has two major contributors: ***i***) electronic structure, and *ii*) nanostructure [23].

4. Conclusions

Nanostructured TiN thin films were successfully obtained at room temperature using a magnetron sputtering. In contrast with those obtained at higher temperatures (200–450 °C), we observed a significant difference, since the nanostructured TiN thin films showed a compact columnar growth, forming agglomerates of nanoparticles and TiN islands with an average grain size of 4.6 m with an average roughness of 1.3 nm and preferential orientation in the [111] direction. This TiN thin films shows a hydrophobic surface Type I and a high electrical conductivity. The combination of the excellent mechanical and electrical properties that can be obtained in this thin films, make it suitable for manufacture of electrodes, for the growth of ferroelectric random access memory (FRAM), the coating of surgical stainless steel, for different uses when the preheated substrate cannot be used.

Conflict of interests

The authors declare that there is no conflict of interests regarding the publication of this paper.

Acknowledgments

This work was economically supported by CONACYT Mexico. The authors thank Javier Martinez for its contribution in the studies of STM. MFM thanks Advanced Nanocomposites Research Group (GINA) at the Materials Engineering Department (DIMAT), University of Concepcion, Concepción-Chile.

References

[1] H. Holleck, J. Vacuum. Sci. Technol. A 4 (1986) 2661–2669.
[2] J.F. Flores, B. Valdez S, M. Schorret, J.J. Olaya, Anti-Corros. Method M 53 (2006) 88–94.
[3] P. De Moor, A. Witvrouw, V. Simona, I. De Wolf, in: Proceedings, SPIE, 3874, 1999, pp. 284–293.
[4] A.J. Perry, R.R. Manory, R. Nowak, D. Rafaja, Vacuum 49 (1998) 89–95.
[5] S. Niyomsoan, W. Grant, D.L. Olson, B. Mishra, Thin Solid Films 415 (2002) 187–194.
[6] J.M. Lackner, W. Waldhauser, R. Ebner, Surf. Coat. Technol. 188 (2004) 519–524.
[7] L. Major, J. Morgiel, B. Major, J.M. Lackner, W. Waldhauser, R. Ebner, L. Nistor, G. Van Tendeloo, Surf. Coat. Technol 200 (2006) 6190–6195.
[8] D.B. Lewis, S.R. Bradbury, M. Sarwar, Wear 197 (1996) 82–88.
[9] B.Y. Mokritskii, Russian Eng. Res. 31 (2011) 164–167.
[10] L.C. Hernández Mainet, L. Ponce, E. Rodriguez, A. Fundora, G. Santana, J. Luis Menchaca, E. Pérez-Tijerina, Nanoscale Res. Lett. 7 (2012) 80–87.
[12] F. Vaz, J. Ferreira, E. Ribeiro, L. Rebouta, S. Lanceros-Mendez, J. A. Mendes, E. Alves, P. Goudeau, J.P. Riviere, F. Ribeiro, I. Moutinho, K. Pischow, J. Rijk, Surf. Coat. Technol. 191 (2005) 317–323.
[12] J. Chang, M.R. Vissers, A.D. Córcoles, M. Sandberg, J. Gao, D. W. Abraham, J.M. Chow, J.M. Gambetta, M.B. Rothwell, G.A. Keefe, M. Steffen, D.P. Pappas, Appl. Phys. Lett. 103 (2013).
[13] Y. Jin, Y.G. Kim, J.H. Kim, D.K. Kim, J. Korean Ceram. Soc 42 (2005) 455–460.
[14] K. Khojier, H. Savaloni, E. Shokrai, Z. Dehghani, N.Z. Dehnavi, J. Theor. Appl Phys (2013).
[15] S.V. Hainsworth, W.C. Soh, Surf. Coat. Tech. 163 (2003) 515–520.
[16] R. Gunda, S.K. Biswas, R. Gunda, S.K. Biswas, J. Am. Ceram. Soc. 88 (2005) 1831–1837.
[17] Y.Y. Guu, J.F. Lin, C. Ai, Wear 194 (1996) 12–21.
[18] B. Subramanian, R. Ananthakumar, M. Jayachandran, Surf. Coat. Technol. 205 (11) (2011) 3485–3492.
[19] C.D. Wanger, W.M. Riggs, L.E. Davis, J.F. Moulder and G.E. Muilenberg, Handbook of X-ray Photoelectron Spectroscopy Perkin-Elmer Corp., Physical Electronics Division, Eden Prairie, Minnesota, USA,.
[20] STRI Guide 92/1: Hydrophobicity Classification Guide, 1992.
[21] K.H. Xue, T.L. Ren, D. Xie, Z. Jia, M.M. Zhang, L.T. Liu, Integr. Ferroelectr. 96 (2008) 19.
[22] A. Malmros, M. Sudow, K. Andersson, N. Rorsman, J. Vac. Sci. Technol. B 28 (2010) 912.
[23] K. Vasu, M. Ghanashyam Krishna, K.A. Padmanabhan, Thin Solid Films 519 (2011) 7702–7706.